Localized magnetic moments in Si:P near the metal-insulator transition

M. Lakner* and H. v. Löhneysen
Physikalisches Institut, Universität Karlsruhe, D-76128 Karlsruhe, Germany

A. Langenfeld and P. Wölfle
Institut für Theorie der Kondensierten Materie, Universität Karlsruhe, D-76128 Karlsruhe, Germany
(Received 11 July 1994)

We report systematic specific-heat measurements of crystalline Si doped with P in the concentration range enclosing the metal-insulator transition, in the temperature range from 40 mK to 3 K and in magnetic fields up to 7 T. The data can be interpreted in terms of a phonon contribution, a term linear in T due to itinerant electrons, which persists even on the insulating side, and an excess contribution ΔC varying sublinearly with temperature. The strong magnetic field dependence of ΔC suggests an interpretation in terms of local magnetic moments. We discuss a theoretical model for the metallic phase, which provides a quantitative description of the concentration of local moments. We show that the temperature power law in zero field can be explained by the Kondo effect.

I. INTRODUCTION

The metal-insulator (MI) transition in heavily-doped semiconductors continues to be a very interesting subject in the physics of disordered solids. In these materials, the disorder stems from the random spatial distribution of donor or acceptor atoms in the single-crystalline host. Recently, the question of localized magnetic moments on the metallic side of the transition has received considerable attention. In particular, for Si:P a number of experimental[1–9] and theoretical[10–14] studies have appeared. In addition, experiments have been reported for Si:B (Ref. 15) and Ge:Sb (Ref. 16) showing the existence of localized moments on the metallic side of the transition. Specific-heat measurements in magnetic fields are particularly well suited to study the interplay between localized and delocalized electrons.[1,2,7,17] With these measurements, the dependence of local moments on the P concentration N could be mapped out systematically for uncompensated Si:P.[7] A major result was that at the critical concentration N_c about 5 to 10% of the P-derived electrons carry a localized moment. Here, in extension of our previous work,[7] we present a rather complete account of the evolution of magnetic moments in uncompensated Si:P as studied experimentally with specific-heat measurements. Concerning compensated Si:P, two different types of samples have been studied addressing the question of local moments. For boron-compensated samples Si:(P,B) local moments in the metallic region were detected by ESR (Ref. 18) and specific-heat measurements.[19] In initially metallic Si:P, which was compensated by acceptor defects introduced by fast neutron irradiation, magnetic moments also survived when annealing the defects partially to come into the metallic region.[20]

The theoretical models to describe magnetic moments span the range from purely phenomenological two-component models[4,21] to numerical calculations of the appearance of magnetic moments in an Anderson-Hubbard model.[11] The second aim of this paper is to deduce on a rather fundamental level the concentration of local magnetic moments in a model of a disordered system incorporating the salient features of Si:P.

The paper is organized as follows. Section II contains some experimental details. The results are presented in Sec. III and are interpreted in terms of a phenomenological two-component model of localized and delocalized electrons in Sec. IV. Section V presents a theoretical derivation of the density of localized moments in a realistic model of metallic Si:P, including a discussion of the Kondo effect on these moments. The contribution to the specific heat of the moments is calculated and shown to compare well with observation.

II. EXPERIMENTAL DETAILS

The samples[22] were grown with the Czochralski method, yielding rods of 54 or 79 mm in diameter with a typical P concentration gradient of $N^{-1}(dN/dx) = 10^{-2}$ cm^{-1} along the axis of the rods. The P concentrations N were determined from the room temperature resistivity using the Thurber scale.[23] For a given sample of $30 \times 20 \times 5$ mm^3 cut from the center of the rod, the concentration variation was appreciably less than 5%. Small bars of the samples were also investigated with electrical-conductivity measurements.[24,25] The magnitude and temperature dependence of the conductivity $\sigma(T)$ is in good agreement with earlier work.[26] [The early rough determination of the critical concentration of our samples quoted as $N_c = 3.2 \times 10^{18}$ cm^{-3} (Ref. 7) was subsequently found to be in error.] A discussion of the critical behavior of the conductivity, including the determination of N_c is given by Stupp *et al.*[24]

The specific heat was measured in a standard ^{3}He/^{4}He

dilution refrigerator with the heat pulse technique. The sample was suspended with nylon threads in a Cu frame firmly connected to the mixing chamber. The addenda (heater and thermometer, and part of the mechanical and electrical links) contributed about 5% at 0.1 K and 20% at 1 K to the total heat capacity in zero magnetic field. A superconducting solenoid provided magnetic fields up to roughly 6 T. Even for low-N samples and in high fields the addenda contribution was always less than 40% except for $N = 0.34 \times 10^{18}$ cm^{-3}, where it rose to 60%.

III. EXPERIMENTAL RESULTS

Figure 1 shows the specific heat C of several Si:P samples spanning two orders of magnitude in concentration, plotted as C/T vs T^2. In this plot, the data above 1.5 K follow straight lines typical of a metal, with a finite intercept γ with the C/T axis (except for the lowest concentrations). For noninteracting electrons $\gamma = (\pi^2/3)k_B^2 N(E_F)$, where $N(E_F)$ is the (single-particle) density of states at the Fermi level. The slope β corresponds to a Debye temperature $\Theta = (1245R/\beta)^{1/3} = (660 \pm 20)$ K, in good agreement with literature data for pure Si. Since our thermometer calibration is not very accurate at high temperatures ($T > 2$ K) because of the very flat R-T characteristic in this range, we do not attach significance to the small apparent variation of β from sample to sample. Figure 2 shows γ vs P concentration N. Also included are earlier data by Kobayashi *et al.*[2] (Note that these authors determined N from the Hall constant $N = 1/R_H e$ without corrections.) Both sets of data vary smoothly across the MI transition with a fast decrease of γ towards zero on the insulating side.

For a parabolic rigid band $N(E_F)$ is given by

$$N(E_F) = v(m^*/\hbar^2\pi^2)(3\pi^2)^{1/3}(n/v)^{1/3}, \qquad (1)$$

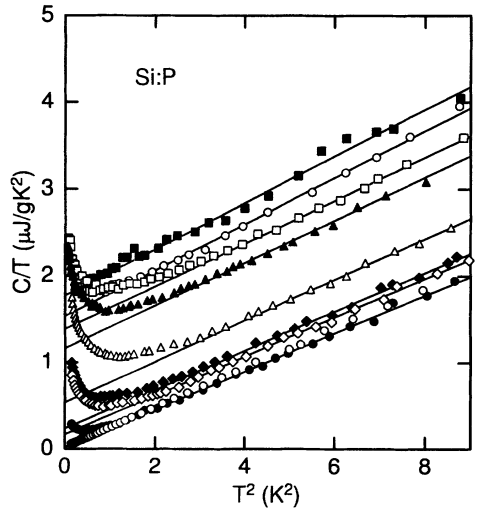

FIG. 1. Specific heat C of Si:P for various P doping concentrations N plotted as C/T versus T^2: ■, 7.3; ○, 4.5; □, 3.6; ▲, 3.3; △, 1.6; ♦, 0.89; ◇, 0.79; •, 0.34; and ○, 0.055×10^{18} cm^{-3}. Solid lines indicate fits of $C/T = \gamma + \beta T^2$. Data below 0.4 K are partly omitted for clarity.

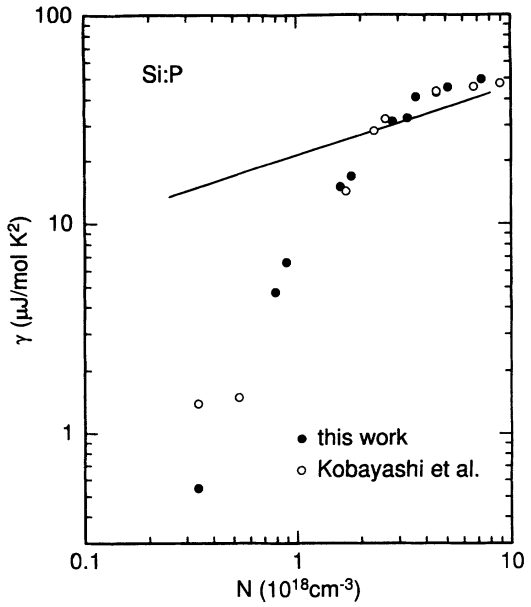

FIG. 2. The specific-heat coefficient γ of the term linear in T versus doping concentration N. Open symbols: data after Kobayashi *et al.* (Ref. 2); closed symbols: this work. Solid line indicates γ according to the nearly-free-electron model Eq. (1).

where n is the electron concentration and v is the valley degeneracy ($v = 6$ for Si). For a parabolic band $N(E_F)$ is proportional to the band effective mass m^* (in general, of course, this need not be true). The solid line is the expectation $\gamma^{(f)}$ for electrons with density $n = N$ with an averaged effective mass $m^* = 0.33m$, where m is the free-electron mass. Above N_c the experimental γ values are close to $\gamma^{(f)}$. This fact has been taken as evidence that the impurity band has merged with the conduction band.[27] However, recent infrared reflectivity measurements on Si:P across the MI transition have clearly shown that the impurity band is energetically separated from the conduction band up to at least $N \approx 2N_c$.[33] Also, it has been suggested that the $N^{1/3}$ dependence of γ above N_c is fortuitous and can be explained if E_F is in the center of an impurity band whose width depends on N and disorder.[28] The above-mentioned optical measurements[33] also have shown that the impurity band is predominantly formed by $1s(A)$ states of the sixfold degenerate valley-orbit split hydrogenic ground state.

A universally accepted explanation for $\gamma(N)$ below N_c does not exist. An early suggestion involving localized electrons[29] must be met with some reservation because the localized electrons give rise to a specific-heat contribution at still lower temperature, which is visible as the upturn in C/T below about 1.5 K and will be discussed below. A possible explanation would be that for $N < N_c$ the sample, because of local fluctuations in concentration, separates into smaller and smaller metallic regions which still may exhibit a finite γ as long as the size of this region containing N_R electrons is such that the average spacing of one-electron levels $\delta \approx E_F/N_R$ is still smaller than the thermal energy, which is > 50 mK $\times k_B$. This

requirement would correspond to $N_R \approx 2000$.

Figures 3–5 show the specific heat C vs T on a log-log scale in order to emphasize the low T region. While the sample with $N = 7.3 \times 10^{18}$ cm^{-3} (and also the sample with $N = 73 \times 10^{18}$ cm^{-3}, not shown) exhibit free-electron behavior $C = \gamma T$ down to the lowest temperatures, strong deviations are observed for small N, in particular, an upturn of C towards a sublinear T dependence. Some indication of such a behavior was reported previously.[4] Unexpectedly, the slope of $C(T)$ changes sign for small N and even becomes negative, i.e., C increases with decreasing T. Of course, since $C \to 0$ for $T \to 0$ this only indicates the existence of an energy scale with C having a maximum at the corresponding temperature, which is shifted to lower and lower energies with decreasing N. Figure 5 demonstrates that this fact is "intrinsic" to the P electron system and is not associated with deep-level impurities such as oxygen. Upon reduction of N further by a factor of 6 from 0.34 to 0.055×10^{18} cm^{-3}, the low-T anomaly is strongly reduced (by roughly a factor of 10). Also, we investigated two samples of float-zone purified Si:P which is expected to have a much lower level of oxygen concentration. Both samples exhibited the same specific heat as the corresponding Czochralski-grown samples.[30]

The specific heat for $B = 0$ for all samples and in the whole temperature range investigated can be described by

$$C = \gamma T + \beta T^3 + \Delta C, \tag{2}$$

where ΔC is shown in Fig. 6. The anomalous contribution to C varies as $\Delta C \sim T^{\alpha_s}$ between our lowest measuring temperature (0.04 K) and 0.3 to 0.4 K, i.e., over almost one decade in T. This allows a reliable determination of the exponent $\alpha_s(N)$ which is shown in Fig. 7. α_s is roughly constant in the metallic range where $\alpha_s \approx 0.2$, decreases with decreasing N, and becomes negative for lowest N. We associate ΔC with the existence of localized magnetic moments which are coupled to the environment by exchange. However, the phenomenological Bhatt-Lee model,[21] where ΔC is explained in a scheme of exchange-coupled pairs with a wide distribution of exchange energies does not allow for negative values of the exponent α_s. Also, the strong decrease of ΔC around 0.5 K suggests a "high-temperature" cutoff at variance with a very wide distribution of exchange energies calculated in the model. Finally, RKKY coupling in the metallic state must also be considered. In Sec. V, we will present a model of partially Kondo screened moments, with a

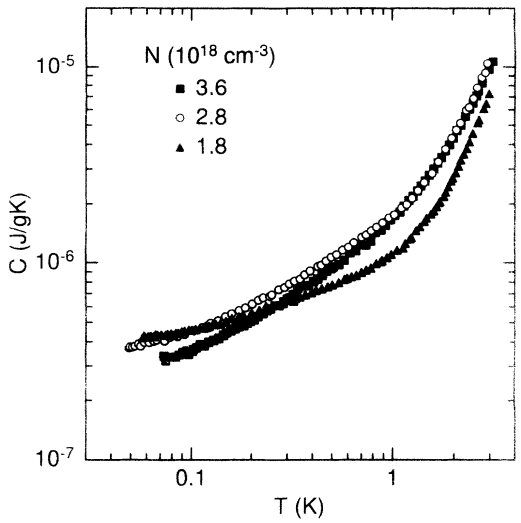

FIG. 4. Log-log plot of specific heat C versus T for intermediate P concentrations in the vicinity of the metal-insulator transition.

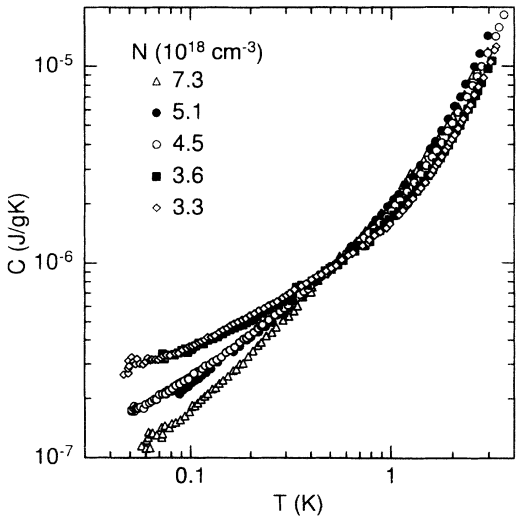

FIG. 3. Log-log plot of specific heat C versus T for the higher P concentrations.

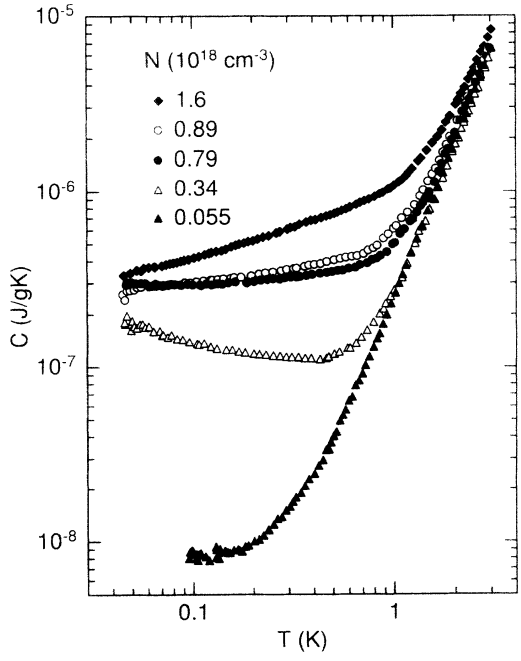

FIG. 5. Log-log plot of specific heat C versus T for the lowest P concentrations.

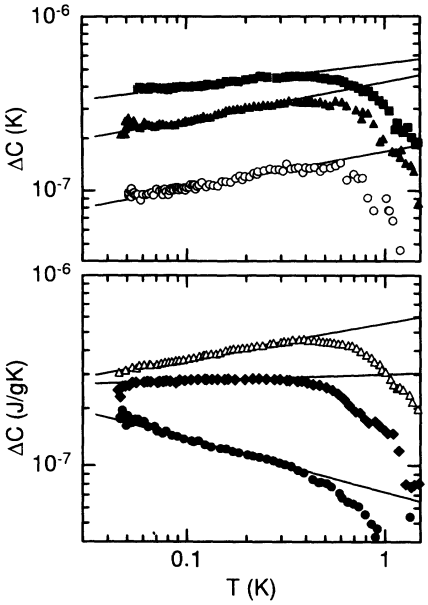

FIG. 6. Log-log plot of the excess specific heat ΔC versus T for various P concentrations N. ○, 4.5; ▲, 3.3; ■, 1.8; △, 1.6; ♦, 0.89; •, 0.34×10^{18} cm^{-3}. Solid line indicates power-law fits.

wide distribution of Kondo temperatures, which appears to account well for the observed behavior in the metallic phase. These points will be discussed further below.

The proof that ΔC is indeed caused by localized moments is provided by the strong magnetic field dependence of C. As the series of Figs. 8 to 11 shows, this dependence becomes gradually stronger with decreasing N. ΔC is suppressed increasingly at low T and, instead, a Schottky-like anomaly develops which is shifted to higher T with increasing B. Also noticeable in Figs. 8 to 11 is the upturn of C at lowest T in high fields. This can be attributed to the Zeeman splitting of ^{31}P nuclei, as inferred from the magnitude and concentration dependence. It is much smaller than expected for ^{29}Si. This shows that even for metallic samples the Korringa relaxation rate for ^{29}Si nuclei is much smaller than the inverse time scale of our specific-heat measurements ($t \sim 1s$), while that for

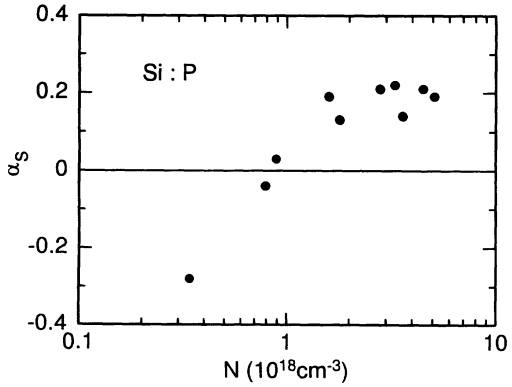

FIG. 7. Exponent α_s of the temperature power-law fitted to ΔC versus doping concentration N.

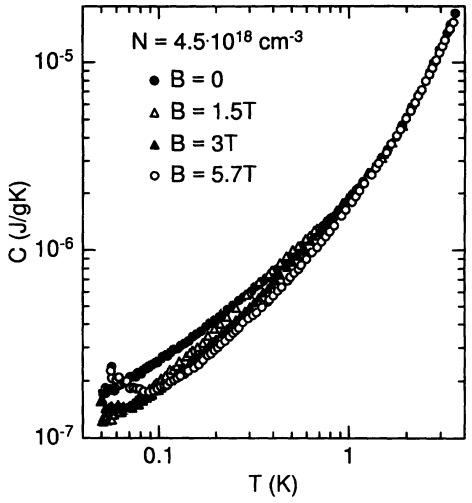

FIG. 8. Log-log plot of specific heat C in magnetic fields versus T at doping concentration $N = 4.5 \times 10^{18}$ cm^{-3}.

^{31}P is comparable to t^{-1}. This is in agreement with NMR experiments on both nuclei.[3,5]

Figures 12 and 13 show for two samples the excess specific heat ΔC in a magnetic field where the contributions $\gamma(B)T+\beta T^3$ have been subtracted. The field dependence of γ has been discussed elsewhere[17] and the observed decrease of $\gamma(B)$ was attributed to a field-induced tendency towards localization. The maximum of ΔC, on the other hand, is seen to increase with B in nice agreement with this idea. However, a change of the specific-heat maximum might also come about because of the large range of exchange couplings, as will be discussed below. The solid lines represent two-level Schottky anomalies, with height directly proportional to the apparent density of local moments $N_{\rm Sch}$. For low fields some deviations occur at low T because of the predominantly antiferromagnetic exchange coupling between localized moments. These deviations are stronger in the metallic than in the insulating

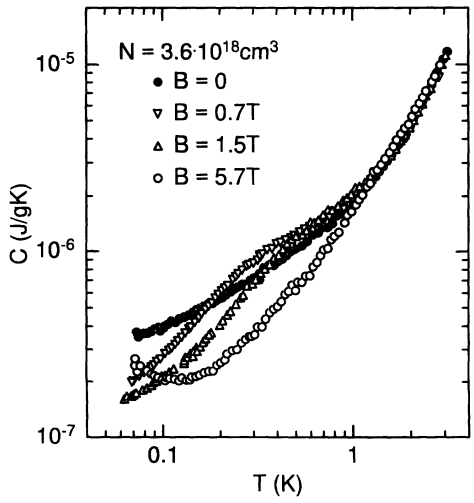

FIG. 9. Log-log plot of specific heat C in magnetic fields versus T at doping concentration $N = 3.6 \times 10^{18}$ cm^{-3}.

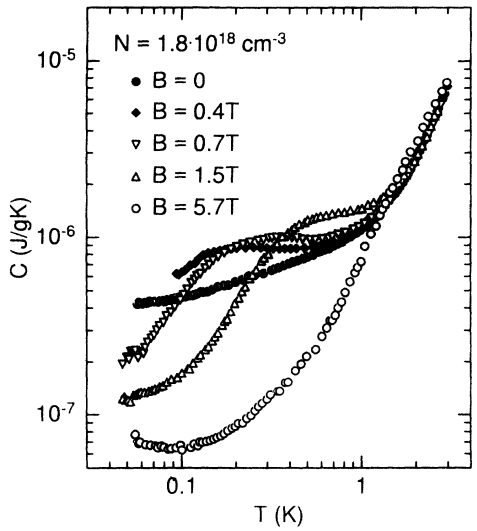

FIG. 10. Log-log plot of specific heat C in magnetic fields versus T at doping concentration $N = 1.8 \times 10^{18}$ cm^{-3}.

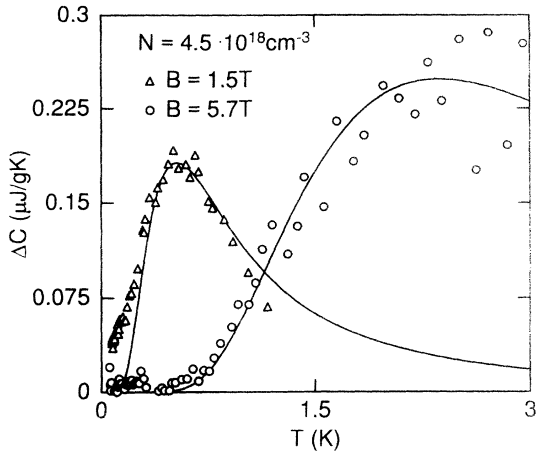

FIG. 12. Excess specific heat ΔC versus temperature for two magnetic fields B at $N = 4.5 \times 10^{18}$ cm^{-3}.

samples. In line with this argument, the effective field obtained from the position of the maximum of the Schottky anomaly $B_{\rm eff} = B + B_i$ is smaller than B, hinting at antiferromagnetic (mean-field) interactions. Figure 14 shows $B_{\rm eff}/B$ as a function of donor concentration for two different fields, $B = 1.5$ and 5.7 T. In spite of the scatter of the data points, a systematic decrease of $B_{\rm eff}/B$ with increasing N can be inferred from the data.

IV. INTERPRETATION OF THE SPECIFIC HEAT IN TERMS OF A TWO-COMPONENT MODEL

The Bhatt-Lee model[21] of localized magnetic moments in doped semiconductors was originally developed for the insulating region, where only localized magnetic moments and no itinerant electrons exist. Due to the random distribution of donor atoms a wide distribution of nearest-neighbor distances and, hence, nearest-neighbor exchange couplings exists. This led Bhatt and Lee to a description of the magnetic properties of doped semiconductors in terms of a hierarchical antiferromagnetic coupling of pairs. For a certain range of exchange energies, the distribution of effective couplings J can be modeled as $P(J) \sim J^{-\alpha_P}$, which leads to power-law behavior in the magnetization and susceptibility, $\chi \sim T^{-\alpha_m}$, and in the specific heat, $C \sim T^{\alpha_s}$, with $\alpha_p = \alpha_m = 1 - \alpha_s$. (In the original literature α has been chosen to represent the exponent of χ and also of C. We choose the above specific notation in order to avoid confusion.) The positive values of α_s for $N \approx N_c$ are in agreement with the Bhatt-Lee model and also with $\alpha_m < 1$ as measured with the magnetic susceptibility.[8] However, the decrease of α_s with decreasing N and the negative value of α_s for 0.34×10^{18} cm^{-3} is unexpected. We previously speculated that this might be due to the neglect of ferromagnetic pairs

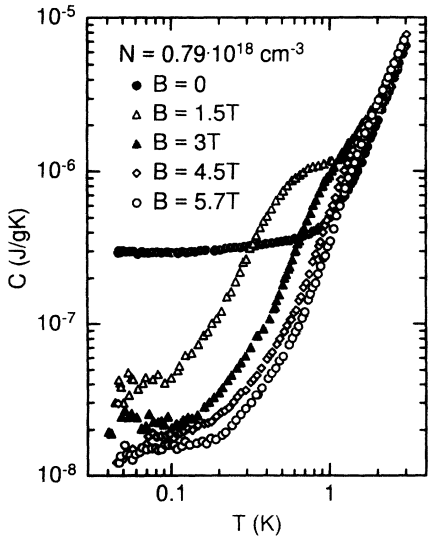

FIG. 11. Log-log plot of specific heat C in magnetic fields versus T at doping concentration $N = 0.79 \times 10^{18}$ cm^{-3}.

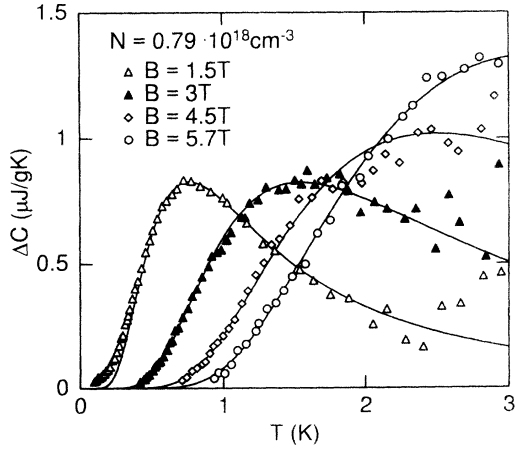

FIG. 13. Excess specific heat ΔC versus temperature for four magnetic fields B at $N = 0.79 \times 10^{18}$ cm^{-3}.

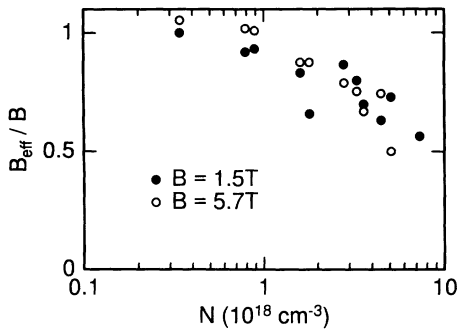

FIG. 14. Effective magnetic field $B_{\rm eff}$ normalized to applied magnetic field B, versus doping concentration N.

and/or of larger clusters.[7] Others[8] have suggested that effective negative α_s values might arise from a crossover between two apparent exponents, since the distribution law $P(J) \sim J^{-\alpha_p}$ is only approximate. A solution to this problem was offered by May,[31] who pointed out that with increasing dilution, the $P(J)$ distribution and also the high-energy cutoff are shifted to lower J, which can result in $\alpha_p > 1$ for an intermediate range of J values and, hence, $\alpha_s < 0$.

We can estimate the density of localized moments N_S from the entropy associated with ΔC for $B = 0$. Of course, this estimate does not account for truly isolated spins which do not contribute to ΔC for $B = 0$. Also, for samples with $\alpha_s < 0$ the extrapolation to $T = 0$ is uncertain. The resulting N_S is plotted against the total number N of electrons in Fig. 15.

In a magnetic field, we have to account for the fact that with increasing B, more and more antiferromagnetic pairs can be aligned by the field. This leads to an increase of the height of the Schottky-like anomaly[31] and thus to a systematic upward shift of $N_{\rm Sch}(5.7\ {\rm T})$ with respect to $N_{\rm Sch}(1.5\ {\rm T})$ in Fig. 15. A recent calculation[32] in terms of a phenomenological small-cluster model supports this interpretation. Furthermore, the systematic difference between $N_S < N_{\rm Sch}$ for $N \lesssim N_c$ and $N_S > N_{\rm Sch}$ for $N \gtrsim N_c$ can be understood qualitatively.[7]

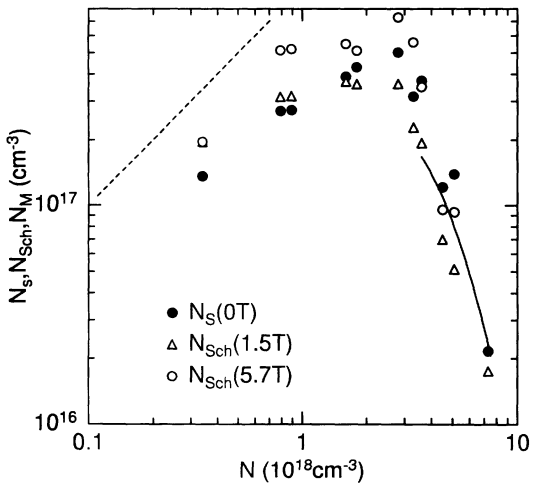

FIG. 15. Concentration of magnetic moments N_s determined experimentally in zero field and $N_{\rm Sch}$ in finite magnetic field versus doping concentration. Dashed line indicates $N_{\rm Sch} = N$ expected in the dilute insulating limit. Solid line gives the concentration of local moments N_M in the metallic phase as calculated in the theory of Sec. V.

V. THEORETICAL MODEL OF MAGNETIC MOMENT FORMATION IN THE METALLIC PHASE

On the metallic side of the metal-insulator transition the donor states have merged to form an impurity band, which is half-filled for uncompensated materials. The simplest model Hamiltonian featuring the essential elements of disorder and Coulomb interaction is the Anderson-Hubbard model,

$$H = \sum_{i\sigma}(\epsilon_i - \mu)n_{i\sigma} + \sum_{ij\sigma} t_{ij}c^+_{i\sigma}c_{j\sigma} + U\sum_i n_{i\uparrow}n_{i\downarrow}, \quad (3)$$

where $c_{i\sigma}(c^+_{i\sigma})$ is the annihilation (creation) operator for an electron with spin projection σ in the lowest state of the dopant atom at site i and $n_{i\sigma} = c^+_{i\sigma}c_{i\sigma}$ is the occupation number operator. We assume that the five excited states generated by the valley-orbit splitting are sufficiently far away that a single-band model is applicable.[34] The host semiconductor does not appear in this except through the fact that the positions $\{i\}$ are those of the Si crystal lattice, and that the effective mass and the interaction are renormalized. The hopping integrals t_{ij} may be approximated [12] as overlap integrals of hydrogen wave functions, $t_{ij} = 2E_0^* \exp(-r_{ij}/a^*)(1 + r_{ij}/a^*)$, with E_0^* and a^* the effective hydrogen binding energy and Bohr radius, respectively. The t_{ij} are random variables according to the randomness of the donor positions. In the following, we will assume the positions i to be the lattice positions of a regular simple hypercubic lattice, with random nearest-neighbor hopping. This is equivalent to keeping only the $2d$ largest hopping amplitudes from any given site in d dimensions and assuming some regularity in the connectivity of the initial random lattice. The on-site energies ϵ_i are approximately equal to the energy ϵ of an isolated dopant level, but fluctuate, in principle, on account of the Coulomb interaction between electrons on different sites. We will assume $\epsilon_i = \epsilon$ in the following. The quantity U describes the on-site Coulomb interaction. It may be estimated by the difference in the ground states of an H^- hydrogenlike ion and the neutral H atom as $U = 0.95E_0^*$, where $E_0^* = (m^*/m)\epsilon^{-2}E_0$ is the ground-state energy of the dopant level (E_0 is the ground-state energy of the hydrogen atom). Using the effective mass $m^* = 0.33m$ and the dielectric constant $\epsilon = 12$ of the Si host material, $E_0^* \simeq 2.4\times10^{-3}$ Ry $= 31$ meV. An estimate of the typical hopping integral at distance $r_0 = N^{-1/3}$ for a density of $N = 5\times10^{18}$ cm^{-3} yields $t = 0.34E_0^*$ and the average value of nearest-neighbor hopping integrals to be considered below is $\langle t\rangle = 0.9E_0^*$. The ratio of Hubbard U to bandwidth is thus $U/12t \simeq 0.08$ for $d =$ three dimensions, which is clearly in the weak-coupling regime.

The excitation gap to the conduction band of $E_G \simeq E_0^*$ estimated in this way, is in reasonable agreement with the well-known value of the ionization energy $E_I = 44$ meV, also obtained from reflectivity measurements[33] at a concentration of 7.3×10^{18} cm^{-3}. The discrepancy of E_I and E_0^* is due to the crystal field splitting of the six valleys of the Si conduction band. In the following, we use the value of $E_0^* = 31$ meV for consistency reasons, rather than scaling the value up to 44 meV. Estimates of the position and width of the impurity "Hubbard bands" indicate that the effective value of U may be somewhat smaller than given above because of the multivalley nature of the impurity band.[35]

The relatively small value of U suggests that a perturbation theory in U might be a good starting point. A Hartree factorization of the interaction term leads to an effective single-particle problem with random hopping. This Hamiltonian has been studied numerically for finite size systems.[11] It was found that some of the magnetic susceptibility eigenvalues turned negative for sufficiently large U, signalling an instability towards local moment formation. An alternative to this numerical treatment is to study a simpler model problem, which can be solved more or less analytically, while still capturing the essential physics.[14]

Observing that the fraction of dopant atoms carrying a local magnetic moment is relatively small, of the order of several percent, it appears reasonable to consider an isolated moment forming in an effective homogeneous medium. The effective Hamiltonian for this impurity problem is given by

$$H = \sum_{\vec{k}\sigma} \epsilon_k c^+_{\vec{k}\sigma} c_{\vec{k}\sigma} + \sum_{\vec{k},\vec{k}'\sigma} V^{\sigma}_{\vec{k}\vec{k}'} c^+_{\vec{k}\sigma} c_{\vec{k}'\sigma}, \tag{4}$$

where the spin-dependent impurity potential is given by

$$V^{\sigma}_{\vec{k}\vec{k}'} = -\frac{1}{2}\sigma M U + V_{\vec{k}} + V_{-\vec{k}'}, \tag{5}$$

and $V_{\vec{k}} = -\epsilon_k - \sum_n \tilde{t}_n e^{-i\vec{k}\cdot\vec{R}_n}$. Here the summation is over the nearest neighbors of the impurity at positions $\vec{R}_n$, and $\tilde{t}_n$ are the random hopping amplitudes to and from site 0 to $\vec{R}_n$. The band energy ϵ_k is given in tight-binding approximation as $\epsilon_k = -2t \sum_{\alpha=1}^{3} \cos k_\alpha r_0$, where $r_0 = N^{-1/3}$ is the lattice parameter of the (fictitious) hypercubic lattice. The local spin occupation number (which is proportional to the magnetization),

$$M = \langle n_{0\uparrow} - n_{0\downarrow} \rangle \tag{6}$$

has to be determined self-consistently. A solution of this problem yields a region of the seven-dimensional parameter space of variables $\tilde{t}_n, U$, where M is finite, i.e., a local magnetic moment exists. The moments are the more stable the higher U and the smaller $\tilde{t}$ is, as one might expect. In particular, for fixed U, there is a critical surface in the six-dimensional parameter space of $\tilde{t}_1, \tilde{t}_2, \ldots, \tilde{t}_6$, which encloses the region of stable moments.

The qualitative explanation for the appearance of moments is that the local level is shifted and split by the interaction U by the amount $\Delta\epsilon = \frac{1}{2}U(1 - \sigma M)$ for spin projection $\sigma = \pm 1$. If the lower level lies sufficiently below the Hartree-shifted levels in the bulk ($\Delta\epsilon_0 = \frac{1}{2}U$), it will be occupied by a single electron and hence carry a magnetic moment, just like in the case of the usual Anderson impurity.[36] We note that this energy shift is caused by a reduced occupation of the impurity site by the unfavorable spin species $n_\downarrow = \frac{1}{2}(1 - M) < \frac{1}{2}$, due to suppressed hopping. However, the total occupation is $n_\uparrow + n_\downarrow = 1$ for the half-filled band case.

Let us now turn to the statistical description of the local moments in the initial problem. In the approximation of independent moments, we may calculate the probability of a donor atom carrying a magnetic moment and hence the density N_M of donors carrying a moment. Assuming the position of the donor atoms to be completely random, the probability for finding the first nearest neighbor at distance r_1, the second one at r_2 and so forth is given by

$$P_{6nn}\{r_n\} = P_1(r_1)\Pi_{n=2}^{6} \times \left[P_n(r_n)\theta(r_n - r_{n-1}) \Big/ \int_{r_n-1}^{\infty} P_n(r'_n)dr'_n \right], \tag{7}$$

where $\theta(x)$ is the step function and $P_n(r)$ is the probability for finding the nth nearest neighbor at distance r,

$$P_n(r) = \frac{4\pi r^2 N}{(n-1)!}\left(\frac{4\pi}{3}r^3 N\right)^{n-1} \exp\left(-\frac{4\pi}{3}r^3 N\right). \tag{8}$$

The probability $P_{6nn}\{r_n\}$ is normalized to unity with respect to integration over all distances $r_n, n = 1, \ldots, 6$.

It is instructive to consider first the distribution of hopping integrals $\tilde{t}_1$ to the nearest neighbor. By inverting the expression of $\tilde{t}_1(r_1)$ in terms of $r_1, r_1(\tilde{t}_1) = a^*[\ell n \frac{t^*}{\tilde{t}_1} + 1]$, where t^* is the hopping integral at distance a^*, we find

$$P_1(\tilde{t}_1) = P_1(r_1(\tilde{t}_1)) \left| \frac{dr_1}{d\tilde{t}_1} \right|. \tag{9}$$

$P_1(\tilde{t}_1)$ is plotted in Fig. 16 for a typical density of donors $N = 5 \times 10^{18}$ cm^{-3}. The distribution is characterized by a broad maximum, a rapid increase at small $\tilde{t}_1$ and

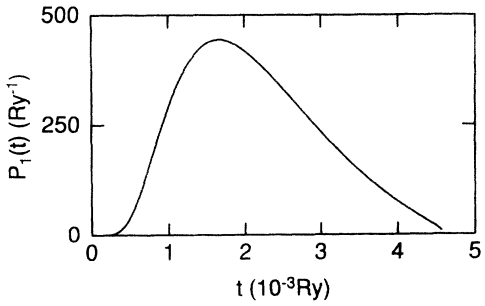

FIG. 16. Probability distribution $P_1(t_1)$ of hopping amplitudes t_1 to the nearest-neighbor site.

an almost linear decrease at higher $\tilde{t}_1$, up to the maximum value $\tilde{t}_{\max} = 2E_0^*$. The density of local moments obtained from applying the mean-field results discussed above is given by

$$N_M = N \int_{S\{\tilde{t}_n\}} P_{6nn}\{r_n(\tilde{t}_n)\} \Pi_{n=1}^{6} \left(\left| \frac{dr_n}{d\tilde{t}_n} \right| d\tilde{t}_n \right), \quad (10)$$

where the integration extends over the region S in parameter space for which $M \neq 0$. In Fig. 15 the density of moments N_M as calculated from (10) is shown as a function of the concentration of dopants N for a value of $U = \langle t \rangle$. Also shown are the experimental estimates of N_M discussed in Sec. III. One observes that the agreement of theory and experiment in the metallic region is very good, except close to the metal-insulator transition. A possible explanation of this deviation is that the distribution of hopping integrals near the transition is modified by the formation of larger clusters weakly coupled to the itinerant part of the sample.[14]

The agreement of the above theoretical estimate with experiment is encouraging. A more stringent test of the theory would be given by the direct comparison of the results of a calculation of observable quantities with experiments. This will be attempted below.

The contribution of the local magnetic moments to the specific heat is determined by their coupling to the heat bath. The principal coupling of a local moment to the environment is the spin-exchange coupling to the conduction electrons. Projecting the Hamiltonian (4) on to the low-energy subspace of Hilbert space analogous to the usual Schrieffer-Wolff transformation, i.e., by eliminating states with no occupancy or double occupancy at the impurity site, one finds an effective spin exchange Hamiltonian. In contrast to the usual Anderson model, here the local spin is coupled to delocalized electron spins on neighboring sites. It may be shown that in the case that the coupling occurs mainly to one nearest-neighbor site (taken to be along the positive x direction), the effective Hamiltonian is given by [14]

$$H = \sum_{\vec{k},\sigma} \epsilon_{\vec{k}} c^+_{\vec{k}\sigma} c_{\vec{k}\sigma} + J_1^{\text{eff}} \sum_{\vec{k}\vec{k}'} \sum_{\sigma\sigma'} \vec{S}_0 \cdot \vec{\tau}_{\sigma\sigma'} c^+_{\vec{k}\sigma} c_{\vec{k}'\sigma'} \times \exp i(k_x - k'_x) a_1, \quad (11)$$

where a_1 is the distance to the nearest neighbor. Note that $\sum_{\vec{k}} c^+_{\vec{k}\sigma} e^{ik_x a_1}$ is the creation operator for an electron at the nearest-neighbor site. Here $\vec{S}_0$ is the spin-$\frac{1}{2}$ operator of the local moment and $\vec{\tau}_{\sigma\sigma'}$ is the vector of Pauli matrices.

The effective exchange coupling has p-wave symmetry and $J_1^{\text{eff}} \sim \frac{1}{2}(\tilde{t}^2/U)$. The s-wave component of the exchange coupling may be shown to vanish. Since J_1^{eff} is positive, the local moment will be screened below the Kondo temperature,

$$T_K = D \exp\left(-\frac{1}{N_0 J_1^{\text{eff}}} \right), \quad (12)$$

where N_0 is the local density of states at the Fermi level at the nearest neighbor, which couples to the impurity, and $D = 6\langle t \rangle$ is half the bandwidth.

From the probability distribution of $\tilde{t}$, one may derive a distribution of Kondo temperatures T_K for the range $0 < T_K < T_M^{\max}$, where $T_K^{\max} = T_K(\tilde{t}_c)$,

$$P_K(T_K) = \frac{N}{N_M} P_1(\tilde{t}(T_K)) \frac{d\tilde{t}}{dT_K}, \quad (13)$$

with $P_1(\tilde{t})$ given by (9)

The distribution $P_K(T_K)$ is dominated by the factor $1/T_K$ originating from the Jacobian factor $d\tilde{t}/dT_K$. A double-logarithmic plot of $P_K(T_K)$ in Fig. 17 reveals that

$$P_K(T_K) = c_0 T_K^{-\alpha_K} \quad (14)$$

for a broad range of T_K values, where $\alpha_K \simeq 0.9$. Here, we used the parameters of the model specified in the text following (3). A power-law behavior of $P_K(T_K)$ leads to a power-law behavior of the specific heat C, due to the fact that $C = \tilde{C}(T/T_K)$ in the Kondo model, where $\tilde{C}(x)$ is a universal function. Neglecting contributions from the boundaries of the power-law regime we find

$$\begin{aligned} C &= c_o \int_{T_K-}^{T_K+} dT_K T_K^{-\alpha_K} \tilde{C}(T/T_K) \\ &= T^{1-\alpha_K} c_o \int_{T_s-}^{T_s+} dx x^{-\alpha_k} \tilde{C}(1/x) \\ &\simeq c_1 T^{1-\alpha_K}. \end{aligned} \quad (15)$$

The exponent of the temperature power law for C, $1 - \alpha_K \simeq 0.1$, agrees reasonably well with the experimentally determined value $\alpha_s \simeq 0.2$. The theoretical exponent α_K depends only weakly on doping, as does the experimental one in the metallic region. Possible sources of the remaining discrepancy are (i) the somewhat uncertain values of the parameters U and N_0, the DOS, and (ii) the effect of antiferromagnetic coupling of the moments by the RKKY interaction. A rough estimate of the RKKY coupling energy $I_{\text{RKKY}} = 3\pi N_0 J^2 (2k_F R)^{-3}$ with $N_0 = (12\langle t \rangle)^{-1}$, $J = 4J_1$, $N = k_F^3/3\pi^2$, $R^3 = N_M^{-1}$ yields $I_{\text{RKKY}} \simeq 0.1$ K for $\tilde{t}$ values at the maximum of the distribution. This indicates that spin correlations mediated by the RKKY interaction may play some role in the experimental temperature regime. Also, the quenching of the Kondo effect by disorder has to be considered. A

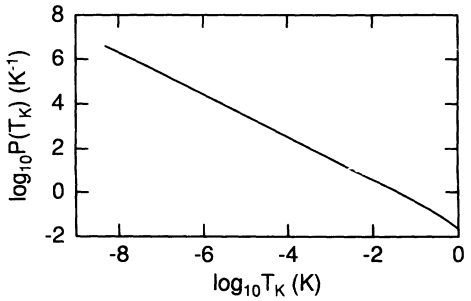

FIG. 17. Log-log plot of the distribution of Kondo temperatures $P(T_K)$ versus T_K, showing power-law behavior.

theoretical study of this effect as well as a more quantitative comparison of theory and experiment, including the effect of a magnetic field is in progress.

VI. CONCLUSIONS

In this paper, we have reported the results of an extensive experimental and theoretical study of local magnetic moments in the heavily doped Si:P system, in a range of doping concentrations including the metal-insulator transition. The existence of local moments is inferred from a specific heat contribution which shows the characteristics of two-level systems when a magnetic field is applied, confirming earlier work. In zero magnetic field the specific heat is analyzed in terms of three contributions, a lattice contribution βT^3, a Fermi liquid contribution γT ascribed to itinerant electrons, and a residual contribution. Surprisingly, the γT contribution appears to be present even in the localized regime close to the transition confirming earlier studies. We conjecture that this contribution is due to conducting islands in the insulating matrix.

The investigation reported in the present paper is focused on the residual part of the specific heat, ΔC. From the entropy associated with ΔC one can estimate the density of local magnetic moments. Theoretically, the existence of local magnetic moments can be derived from a one-band model of weakly correlated electrons hopping between statistically distributed donor sites. In an effective medium approximation, we determine the criterium for the existence of moments on isolated sites. The number of moments at given donor concentration may be estimated and is found to agree well with the data. It is found that within the temperature range investigated, ΔC can be represented by a temperature power law, T^{α_s}. In the metallic phase, $\alpha_s \simeq 0.2$, approximately independent of doping concentration. We show that a contribution of this type is generated by a statistical ensemble of local magnetic moments, exchange coupled to the conduction electron system. For the simplest model, with realistic parameter values, we find $\alpha_s \simeq 0.1$. On the insulating side of the transition, the experimentally determined exponent α_s is found to decrease continuously with decreasing doping concentration, down to negative values ~ -0.3 at the lowest concentration measured. In this regime, a model of exchange-coupled spins with a wide distribution of coupling constants should be appropriate. As shown by Bhatt and Lee,[21] the successive freezing out of singlet pairs, as the temperature is lowered, should lead to a temperature power law with, however, a positive exponent α_s.

The measured specific heat shows rich behavior as a function of magnetic field, generally consistent with the notion of spin-singlet systems and single spins, which are broken up and Zeeman split by the magnetic field. A detailed comparison with theory has not been attempted here. Work in this direction is in progress.

Although the concept of local magnetic moments in doped semiconductors near the metal-insulator transition is confirmed by the present study, a number of unresolved issues remain. First, on the metallic side the nature of the interaction of the moments is not yet clarified beyond doubt. The model of partially Kondo screened impurities presented here appears to give a reasonable account of the data at least in zero magnetic field. However, the role of the indirect or also the direct exchange interaction deserves further clarification. A quantitative comparison with the observed magnetic field dependence should allow us to distinguish the two contributions.

On the insulating side, the observed negative exponent α_s of ΔC needs further consideration. Here also the magnetic field dependence should help to identify the relevant processes.

As a final remark, we emphasize that the formation of local magnetic moments is not induced by or related to the metal-insulator transition. This is apparent from the noncritical behavior of the density of moments across the transition (see Fig. 15). This phenomenon is a short distance effect and should not be mixed up with a possible vanishing of the spin diffusion coefficient at or near the MI transition. On the other hand, the existence of local moments may influence the critical behavior.

ACKNOWLEDGMENTS

We thank S. Wagner for her help with some specific-heat measurements. This work has been supported by Deutsche Forschungsgemeinschaft through Sonderforschungsbereich 195.

* Present address: ABB Corporate Research, CH-5405 Baden-Dättwil, Switzerland.

[1] J.R. Marko, J.P. Harrison, and J.D. Quirt, Phys. Rev. **B 10**, 2448 (1974).
[2] N. Kobayashi, S. Ikehata, S. Kobayashi, and W. Sasaki, Solid State Commun. **24**, 67 (1977); **32**, 1147 (1979).
[3] M.A. Paalanen, S. Sachdev, R.N. Bhatt, and A.E. Ruckenstein, Phys. Rev. Lett. **57**, 2061 (1986).
[4] M.A. Paalanen, J.E. Graebner, R.N. Bhatt, and S. Sachdev, Phys. Rev. Lett. **61**, 597 (1988).
[5] H. Alloul and P. Dellouve, Phys. Rev. Lett. **59**, 578 (1987).
[6] A. Roy and M.P. Sarachik, Phys. Rev. B **37**, 5531 (1988).
[7] M. Lakner and H. v. Löhneysen, Phys. Rev. Lett. **63**, 648 (1989).
[8] Y. Ootuka and N. Matsunaga, J. Phys. Soc. Jpn. **59**, 1891 (1990).
[9] N. Matsunaga and Y. Ootuka, J. Phys. Soc. Jpn. **62**, 1745 (1993).
[10] S. Sachdev, Phys. Rev. B **39**, 5297 (1989).
[11] M. Milovanovic, S. Sachdev, and R.N. Bhatt, Phys. Rev. Lett. **63**, 82 (1989).
[12] R.N. Bhatt and D.S. Fisher, Phys. Rev. Lett. **68**, 3072 (1992).
[13] V. Dobrosavljevic and G. Kotliar, Phys. Rev. Lett. **71**,

3218 (1993).
[14] A. Langenfeld and P. Wölfle, Ann. Phys. (Leipzig) (to be published).
[15] M.P. Sarachik, A. Roy, and R.N. Bhatt, Solid State Commun. **60**, 513 (1986).
[16] Y. Ootuka and N. Matsunaga, Solid State Commun. **75**, 255 (1990); C. Paschke, H.v. Löhneysen, and Y. Ootuka, Phys. Rev. B **49**, 2170 (1994).
[17] H. v. Löhneysen and M. Lakner, Physica **165&166B**, 285 (1990).
[18] M.J. Hirsch, D.F. Holcomb, R.N. Bhatt, and M.A. Paalanen, Phys. Rev. Lett. **68**, 1418 (1992).
[19] S. Wagner, M. Lakner, and H. v. Löhneysen (unpublished).
[20] M. Straub, K. Kirch, and H. v. Löhneysen, Z. Phys. B **95**, 31 (1994).
[21] R.N. Bhatt and P.A. Lee, Phys. Rev. Lett. **48**, 344 (1982).
[22] The samples were provided by D.W. Zulehner, Wacker Chemitronic, Burghausen, Germany.
[23] W.R. Thurber, R.L. Matthis, Y.M. Liu, and J.J. Filliben, J. Electrochem. Soc. **127**, 1807 (1980).
[24] H. Stupp, M. Hornung, M. Lakner, O. Madel, and H. v. Löhneysen, Phys. Rev. Lett. **71**, 2634 (1993).
[25] H. v. Löhneysen and M. Welsch, Phys. Rev. B **44**, 9045 (1991).
[26] T.F. Rosenbaum, R.F. Milligan, M.A. Paalanen, G.A. Thomas, and R.N. Bhatt, Phys. Rev. B **27**, 7509 (1983).
[27] S.R. Meyer and F.J. Bartoli, Philos. Mag. Lett. **56**, 69 (1987).
[28] M. Kaveh and A. Liebert, Philos. Mag. Lett. **58**, 247 (1988).
[29] K.A. Chao and A. Ferreira da Silva, Phys. Rev. B **19**, 4125 (1979).
[30] S. Wagner, H. v. Löhneysen, and W. Schröter (unpublished).
[31] C. May, Ph.D. thesis, Max-Planck-Institut Stuttgart, 1992.
[32] M.J.R. Hock and C. Kasl, Phys. Rev. B **49**, 2331 (1994).
[33] A. Gaymann, H.P. Geserich, and H. v. Löhneysen, Phys. Rev. Lett. **71**, 3681 (1993).
[34] R.N. Bhatt and S. Sachdev, Phys. Rev. B **34**, 3520 (1986).
[35] R.N. Bhatt and T.M. Rice, Phys. Rev. B **23**, 1920 (1981).
[36] P.W. Anderson, Phys. Rev. **124**, 41 (1961); P. Wolff, *ibid.* **124**, 1030 (1961).